Key Process of the Photocatalytic Reduction of CO_2 Using [Re(4,4′-X_2-bipyridine)$(CO)_3PR_3]^+$ (X = CH_3, H, CF_3; PR_3 = Phosphorus Ligands): Dark Reaction of the One-Electron-Reduced Complexes with CO_2

Kazuhide Koike,*,† Hisao Hori,*,† Masakazu Ishizuka,† Jeremy R. Westwell,† Koji Takeuchi,† Takashi Ibusuki,† Kengo Enjouji,‡ Hideo Konno,‡ Kazuhiko Sakamoto,‡ and Osamu Ishitani*,‡

Photoenergy Application Laboratory, National Institute for Resources and Environment, 16-3 Onogawa, Tsukuba, Ibaraki 305, Japan, and Graduate School of Science and Engineering, Saitama University, 255 Shimo-Okubo, Urawa 338, Japan

Received July 17, 1997[⊗]

Reduction of CO_2 to CO was efficiently photocatalyzed by [Re(4,4′-X_2bpy)$(CO)_3PR_3]^+$ (X = H, Me; PR_3 = $P(OEt)_3$, $P(O\text{-}i\text{-}Pr)_3$) in quantum yields of 0.16−0.20. Complexes with CF_3 as X or trialkylphosphine as PR_3 have much lower photocatalytic ability. One-electron-reduced species of the complexes, which were produced by the photoinduced electron-transfer reaction with triethanolamine, reacted with CO_2 in the dark with rate constants of 3.5×10^{-4}−1.9×10^{-2} M^{-1} s^{-1}. The faster the rate of this process, the higher the quantum yield of CO formation. The calculated amount of CO formation, based on the assumption that the process gives CO quantitatively, was similar to the actually observed amount under various conditions. This is consistent with the thermal process being one of the rate-limiting steps in the photocatalyzed reduction of CO_2 by the rhenium complexes.

Introduction

Photocatalysis by rhenium polypyridine complexes such as $XRe(bpy)(CO)_3$ (X = Cl, Br; bpy = 2,2′-bipyridine), especially for CO_2 reduction, has received a great deal of attention because of not only the high efficiencies but also the capability of the two-electron-transfer mediation without the assistance of any cocatalyst.[1−8] Several mechanistic studies have shown that the CO_2 reduction is initiated by electron transfer from an electron donor, *i.e.*, triethanolamine (TEOA) or triethylamine, to the excited rhenium complex to produce the one-electron-reduced (OER) rhenium species.[7,9−12] Although loss of chloride anion probably from the OER species was reported,[2,13,14] it is a competitive deactivation process in the photocatalysis.[2] Little is known about other chemical properties of the OER complexes, and the identity of the species which reacts with CO_2 in the photocatalytic cycle remains unknown. One problem is the instability of the OER species: the lifetime of $[BrRe(bpy)(CO)_3]^-$ is 10 s under an argon atmosphere and 6 s under a carbon dioxide atmosphere, even in the presence of Br^-.[15]

Recently, $[Re(bpy)(CO)_3\{P(OEt)_3\}]^+$ was found to work as an efficient photocatalyst for CO_2 reduction, the associated OER complex being much more stable than other related rhenium complexes due to the strong π-accepting ability of the phosphorus ligand.[7,14] Systematic comparison of the photocatalytic behavior of rhenium complexes, which have various phosphorus ligands and substituents on the 4,4′-positions of the bpy ligand, will provide important information about the properties of the OER complexes and the mechanism of the photocatalytic reduction of CO_2.

In this paper, we report the spectroscopic properties and the reactivities of the OER species of the rhenium complexes [Re(4,4′-X_2-bipyridine)$(CO)_3PR_3]^+$ (X = H, PR_3 = $P(n\text{-}Bu)_3$ (**1**$^+$), PEt_3 (**2**$^+$), $P(O\text{-}i\text{-}Pr)_3$ (**3**$^+$), $P(OEt)_3$ (**4**$^+$), $P(OMe)_3$ (**5**$^+$); X = CH_3, R = $P(OEt)_3$ (**6**$^+$); X = CF_3, R = $P(OEt)_3$ (**7**$^+$)). An important finding is that the OER complexes can react with CO_2 in the dark as a key process in the photocatalytic reduction of CO_2.

Experimental Section

General Procedures. The redox potentials of the complexes **1**$^+$−**7**$^+$ were measured in MeCN solutions containing $n\text{-}Bu_4NClO_4$ (0.1 M) as the supporting electrolyte by a cyclic

† National Institute for Resources and Environment.
‡ Saitama University.
[⊗] Abstract published in *Advance ACS Abstracts,* December 1, 1997.

(1) Carzafferri, G.; Hadener, K.; Li, J. *J. Photochem. Photobiol. A* **1992**, *64*, 259.
(2) Hawecker, J.; Lehn, J.-M.; Ziessel, R. *Helv. Chim. Acta* **1986**, *69*, 1990.
(3) Hukkanen, H.; Pakkanen, T. T. *Inorg. Chim. Acta* **1986**, *114*, L43.
(4) Ishitani, O.; Namura, I.; Yanagida, Y.; Pac, C. *J. Chem. Soc., Chem. Commun.* **1987**, 1153−1154.
(5) Pac, C.; Ishii, K.; Yanagida, S. *Chem. Lett.* **1989**, 765.
(6) Pac, C.; Kaseda, S.; Ishii, K.; Yanagida, S. *J. Chem. Soc., Chem. Commun.* **1991**, 787.
(7) Hori, H.; Johnson, F. P. A.; Koike, K.; Ishitani, O.; Ibusuki, T. *J. Photochem. Photobiol. A: Chem.* **1996**, *96*, 171−174.
(8) Hori, H.; Johnson, F. P. A.; Koike, K.; Takeuchi, K.; Ibusuki, T.; Ishitani, O. *J. Chem. Soc., Dalton Trans.* **1997**, 1019.
(9) Kalyanasundaram, K. *J. Chem. Soc., Faraday Trans. 2* **1986**, *82*, 2401.
(10) Kutal, C.; Weber, M. A.; Ferraudi, G.; Geiger, D. *Organometallics* **1985**, *4*, 2161.
(11) Kutal, C.; Corbin, A. J.; Ferraudi, G. *Organometallics* **1987**, *6*, 553.
(12) Ishitani, O.; George, M. W.; Ibusuki, T.; Johnson, F. P. A.; Koike, K.; Nozaki, K.; Pac, C.; Turner, J. J.; Westwell, J. R. *Inorg. Chem.* **1994**, *33*, 4712−4717.
(13) Christensen, P.; Hamnett, A.; Muir, A. V. G.; Timney, J. A. *J. Chem. Soc., Dalton Trans.* **1992**, 1455−1463.
(14) Johnson, F. P. A.; George, M. W.; Hartle, F.; Turner, J. J. *Organometallics* **1996**, *15*, 3374−3387.
(15) Ishitani, O.; Pac, C. Unpublished results.

S0276-7333(97)00608-0 CCC: $14.00

Table 1. Photochemical Reduction of CO_2 Using 1^+-7^+ as a Photocatalyst,[a] Reaction of the OER Species 1−7 with CO_2, and the Properties of 1^+-7^+

$[Re(X_2bpy)(CO)_3(PR_3)]^+$			irrad				k_q[f]/10^8	k_1[g]/10^8			
a$^+$	X	PR_3	time/h	TN[b,c]	Φ_{CO}[c,d]	$[\mathbf{a}^+]_{re}$[e]/mM	M^{-1} s^{-1}	M^{-1} s^{-1}	χ[h]	θ[i]/deg	$-E_{1/2}$[j]/V
$\mathbf{1}^+$	H	P(*n*-Bu)$_3$	13	0.65	0.013	0.07	3.9	10.7	5.25	132	1.39[k]
$\mathbf{2}^+$	H	PEt_3	13	0.83	0.024	0.25	4.1	3.5	6.30	132	1.39[k]
$\mathbf{3}^+$	H	P(O-*i*-Pr)$_3$	13	6.2	0.20	0.30	8.6	94.2	19.05	130	1.44[k]
$\mathbf{4}^+$	H	P(OEt)$_3$	13	5.9	0.16	0.29	11.0	56.0	21.6	109	1.43[k]
$\mathbf{5}^+$	H	P(OMe)$_3$	13	5.5	0.17	*l*	14.0	60.0	24.1	107	1.41[k]
$\mathbf{6}^+$	Me	P(OEt)$_3$	17	4.1	0.18	0	6.8	186			1.55
$\mathbf{7}^+$	CF_3	P(OEt)$_3$	17	0.10	0.005	0.85	8.8	5.2			1.03

[a] A 4 mL DMF−TEOA solution containing the complex (2.6 mM) was irradiated at 365 nm. [b] Turnover numbers of CO formation based on the complexes used. [c] Light intensity was 1.27×10^{-8} einstein s^{-1}. [d] Quantum yield of CO formation. [e] The residual complexes in the solution after the irradiation. [f] Emission quenching rate constants by TEOA in DMF. [g] Second-order rate constants of the reaction between the OER complexes and CO_2 (0.139 M) (see text). [h] Tolman's χ.[27,28] [i] Cone angles of the phosphorus ligands. [j] Redox potentials for **a**/**a**$^+$ in MeCN containing 0.1 M *n*-Bu_4NClO_4: scan rate 200 mV s^{-1} with a glassy-carbon working electrode vs $Ag/AgNO_3$ (0.1 M). [k] From ref 22. [l] $\mathbf{5}^+$ could not be determined by HPLC.

voltammetric technique using a BAS 100W electrochemical analyzer with a glassy-carbon working electrode, a $Ag/AgNO_3$ reference electrode, and a Pt counter electrode. UV/vis and IR absorption spectra were recorded on Photal MCPD-1000 and JEOL JIR-6500 spectrometers, respectively. A flow electrolytic technique, described in detail elsewhere,[12] was employed to measure UV/vis and IR spectra of the OER complexes. The emission spectra were measured at 25 °C using a Hitachi F-3000 fluorescence spectrometer. ^{1}H NMR and ^{13}C NMR spectra were recorded on a Bruker AC 300P NMR spectrometer at 25 °C. Chemical shifts (δ, ppm) are downfield from the internal TMS calibration. A laser flash photolysis apparatus was employed to measure the emission lifetimes of the excited complexes and determine the quenching rate constants corresponding to reaction with TEOA. Details of this system are described elsewhere.[12] The principal force constants of CO (k_{ax} and k_{eq}) were calculated using energy factored force field (EFFF) analysis based on the approximation that the two interaction constants (k_{axeq} and k_{eqeq}) are the same.[16−20]

Materials. Dimethylformamide (DMF) was distilled under reduced pressure (~10 Torr) in the presence of 4A molecular sieves, and TEOA was distilled under reduced pressure (~0.1 Torr) before use. $ClRe(4,4'\text{-}X_2bpy)(CO)_3$ compounds were prepared according to the literature method.[21] The PF_6^- salts of $\mathbf{1}^+-\mathbf{5}^+$ were prepared according to the methods described elsewhere.[22] Preparation methods of $\mathbf{6}^+PF_6^-$ and $\mathbf{7}^+PF_6^-$ are as follows.

[Re(4,4′-Me$_2$bpy)(CO)$_3${P(OEt)$_3$}]$^+$PF$_6^-$ ($\mathbf{6}^+PF_6^-$). The complex $ClRe(4,4'\text{-}Me_2bpy)(CO)_3$ (0.858 g) and $Ag^+CF_3SO_3^-$ (0.500 g) were dissolved in 150 mL of tetrahydrofuran and refluxed in the dark under an argon atmosphere for 3 h. The precipitated silver chloride was filtered off, and triethyl phosphite (1 mL) was added to the filtrate. The solution was kept at room temperature for 12 h; then the solvent was evaporated. The resulting yellow solid was washed three times with ether, and recrystallization was achieved with dichloromethane−ether. The yield of $[Re(4,4'\text{-}Me_2bpy)(CO)_3\{P(OEt)_3\}]^+CF_3SO_3^-$ was 93%. The $CF_3SO_3^-$ salt was dissolved in a small amount of methanol, and 5 mL of saturated methanol solution of NH_4PF_6 was added. Water (10 mL) was added dropwise to precipitate the pale yellow product $\mathbf{6}^+PF_6^-$, which was collected by filtration, washed with water, and then dried in vacuo. ^{1}H NMR (300 MHz, $CDCl_3$): δ 8.84 (2H, s, Me_2bpy H^3,H$^{3'}$), 8.65 (2H, d, J = 5.2 Hz, Me_2bpy H^6,H$^{6'}$), 7.38 (2H, d, J = 5.7 Hz, Me_2bpy H^5,H$^{5'}$), 3.78 (6H, quint, J = 7.0 Hz and $J_{H,P}$ = 7.0 Hz, OCH_2), 2.68 (6H, s, Me_2bpy CH_3), 1.04 (9H, t, J = 7.0 Hz, OEt CH_3). ^{13}C NMR (75.5 MHz, $CDCl_3$): δ 193.5 (d, J_{P-C} = 12.2 Hz, equatorial CO), 187.7 (d, J_{P-C} = 99.0 Hz, axial CO), 156.0 (Me_2bpy C^2,C$^{2'}$), 154.1 (Me_2bpy C^4,C$^{4'}$), 152.1 (Me_2bpy C^6,C$^{6'}$), 128.4 and 126.6 (Me_2bpy C^3,C$^{3'}$ and Me_2bpy C^5,C$^{5'}$), 62.4 (d, J_{P-C} = 7.3 Hz, OC), 21.4 (Me_2bpy CH_3), 15.8 (d, J_{P-C} = 5.8 Hz, CH_3). IR (MeCN): ν(CO) 2045, 1958, 1926 cm^{-1}. Anal. Calcd for $\mathbf{7}^+CF_3SO_3^-$, $C_{22}H_{27}N_2O_9F_3PSRe$: C, 34.33; H, 3.54; N, 3.64. Found: C, 34.11; H, 3.32; N, 3.35.

[Re{4,4′-(CF$_3$)$_2$bpy}(CO)$_3${P(OEt)$_3$}]$^+$PF$_6^-$ ($\mathbf{7}^+PF_6^-$). The complex $\mathbf{7}^+PF_6^-$ was synthesized using a procedure analogous to that given for $\mathbf{6}^+PF_6^-$, except that $ClRe\{4,4'\text{-}(CF_3)_2bpy\}(CO)_3$ was used as a starting material and the solution was refluxed for 4 h after the addition of triethyl phosphite. Yield: 85%. ^{1}H NMR (300 MHz, $CDCl_3$): δ 9.15 (2H, d, J = 5.8 Hz, $(CF_3)_2$bpy H^6,H$^{6'}$), 8.78 (2H, s, $(CF_3)_2$bpy H^3,H$^{3'}$), 7.88 (2H, d, J = 4.7 Hz, $(CF_3)_2$bpy H^5,H$^{5'}$), 3.79 (6H, quint, J = 7.0 Hz and $J_{H,P}$ = 7.0 Hz, OCH_2), 0.98 (9H, t, J = 7.0 Hz, CH_3). IR (MeCN): ν(CO) 2053, 1971, 1935 cm^{-1}. Anal. Calcd for $\mathbf{7}^+PF_6^-$, $C_{21}H_{21}N_2O_6F_{12}P_2Re$: C, 28.87; H, 2.42; N, 3.21. Found: C, 28.85; H, 2.24; N, 2.99.

Photocatalytic Reaction. A 4 mL DMF−TEOA (5:1 v/v) solution containing each of the rhenium complexes (2.6 mM) was introduced into a quartz cubic cell (7 mL volume) and bubbled with pure CO_2 for 20 min before the cell was sealed using a rubber septum (Aldrich). The sample solution was kept at 20 ± 1 °C and irradiated at 365 nm using a 500 W high-pressure mercury lamp with a band-pass filter (Asahi-Bunko). A gas sample was taken using a gastight syringe, and the formation of the reaction products, i.e., CO and H_2, was measured by GC−TCD. The incident light intensity into the cell was 1.27×10^{-8} einstein s^{-1}, which was determined using a $K_3Fe(C_2O_4)_3$ actinometer.

Kinetics. The UV/vis absorption spectral change of the solution was monitored using a Photal MCPD 1000 spectrophotometer connected to the photochemical cell through optical fibers. The concentration of the OER complexes was calculated from the absorbance at the absorption band maximum around 505 nm because the parent species $\mathbf{1}^+-\mathbf{7}^+$ and the successive reaction products of the OER species do not have any absorption in this region.

Results

Photocatalytic Reduction of CO_2. It was confirmed that $\mathbf{3}^+-\mathbf{6}^+$ photocatalyze the selective reduction of CO_2 to CO with a very small amount of hydrogen formation. The results are summarized in Table 1. The turnover numbers (TN) of the CO formation were larger than 5.5 for $\mathbf{3}^+-\mathbf{5}^+$ and 4.1 for $\mathbf{6}^+$ after 13 h of

(16) Cotton, F. A.; Kraihanzel, C. S. *J. Am. Chem. Soc.* **1962**, *84*, 4432.
(17) Cotton, F. A.; Musco, A.; Yagupsky, G. *Inorg. Chem.* **1967**, *6*, 1357.
(18) Cotton, F. A. *Inorg. Chem.* **1968**, *7*, 1683.
(19) Dalton, J.; Paul, I.; Smith, J. G.; Stone, F. G. A. *J. Chem. Soc. A* **1968**, 1208.
(20) Jones, L. H. *Inorg. Chem.* **1967**, *6*, 1269.
(21) Wrighton, M. S.; Morse, D. L. *J. Am. Chem. Soc.* **1974**, *96*, 998.
(22) Hori, H.; Koike, K.; Ishizuka, M.; Takeuchi, K.; Ibusuki, T.; Ishitani, O. *J. Organomet. Chem.* **1997**, *530*, 169.

Table 2. Spectroscopic Properties of the OER Complexes 1−7

OER complexes	UV/vis[a]			IR[b]	
	λ_{max}/nm[c]	T_{max}[d]/s	A_{max}[e]	ν_{CO}[f]/cm^{-1}	$-\Delta\nu_{CO}$[g]/cm^{-1}
1	345, 380−395, 458, 480, 507, >866	600	1.14	1885, 1910, 2011	33.8, 36.6, 24.1
2	343, 383, 393, 458, 480, 507, ∼840 (sh), >866	600	1.22	1887, 1912, 2011	31.9, 34.7, 25.1
3	385, 393, 455, 478, 505, >866	270	0.81	1894, 1925, 2020	30.8, 33.8, 25.1
4	382, 394, 456, 478, 506, ∼840 (sh), >866	180	0.88	1898, 1928, 2022	29.9, 34.7, 25.1
5	383, 394, 455, 479, 504, 843, >866	320	0.87	1899, 1932, 2025	31.8, 32.7, 24.1
6	331, 397, ∼450 (sh), 485, 516, ∼730 (sh), 818	260	0.97	1896, 1926, 2021	28.9, 33.7, 23.2
7	347, 383, 465, 472, 507, >866	270	1.10	1906, 1937, 2030	29.9, 32.8, 24.1

[a] The OER complexes were photochemically produced in a DMF−TEOA (5:1 v/v) solution. [b] The OER complexes were electrochemically produced in an MeCN solution containing 0.1 M n-Bu_4NClO_4. [c] The UV/vis absorption maxima of the OER complexes. [d] The time when the absorbance of the OER complex reached a maximum. [e] The maximum absorbance of the OER complex absorption band around 505 nm at the time T_{max}. [f] The IR absorption maxima of the OER complexes. [g] The CO stretching band shifts of the OER complexes from the corresponding $\mathbf{1}^+$−$\mathbf{7}^+$ complexes.[22]

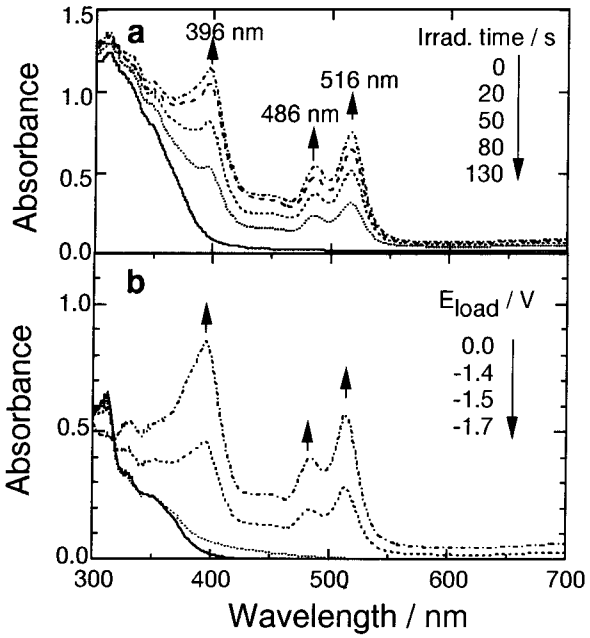

Figure 1. (a) UV/vis absorption change of a DMF−TEOA (5:1 v/v) solution containing $\mathbf{6}^+$ (0.26 mM) during photoirradiation (365 nm) under a CO_2 atmosphere. (b) UV/vis absorption change of an MeCN solution containing $\mathbf{6}^+$ (0.55 mM) during electrolysis at various potentials vs $Ag/AgNO_3$ under an Ar atmosphere.

irradiation (Table 1). On the other hand, the photoreduction of CO_2 by $\mathbf{1}^+$, $\mathbf{2}^+$, and $\mathbf{7}^+$ occurred inefficiently with a TN of less than unity. After the photoreaction, 24−50% of $\mathbf{1}^+$−$\mathbf{5}^+$ and $\mathbf{7}^+$ still remained in the solution, but more than 90% of $\mathbf{6}^+$ was decomposed.[23] Presumably, the relatively low TN of $\mathbf{6}^+$ might be mainly attributable to the instability of the complex in the photocatalytic cycle, whereas $\mathbf{1}^+$, $\mathbf{2}^+$, and $\mathbf{7}^+$ seem to inherently lack photocatalytic ability. It was also found that the quantum yields of CO formation are strongly dependent upon the PR_3 and X_2bpy ligands, as shown in Table 1. $\mathbf{3}^+$−$\mathbf{6}^+$ showed fairly high quantum yields of CO formation (0.16−0.20 with light intensity of 1.27 × 10^{-8} einstein s^{-1}).

Long irradiation caused decomposition of the complexes and a drop in the CO formation rate. It is noteworthy that, in the cases of $\mathbf{3}^+$ and $\mathbf{4}^+$, the formate complex [Re(bpy)$(CO)_3$(OCHO)] was produced in 24% and 73% yields based on the amount of the consumed complexes respectively after 4 h of irradiation. The formate complex has a much lower photocatalytic activity than $\mathbf{3}^+$ and $\mathbf{4}^+$.[2,7,8] These results show that loss of the phosphorus ligand is one of the main deactivation channels of the photocatalysis.

Photochemical and Electrochemical Formation of the OER Complexes. All of the rhenium complexes $\mathbf{1}^+$−$\mathbf{7}^+$ are emissive from the triplet metal-to-ligand charge-transfer (^{3}MLCT) excited state at room temperature.[22] The emission of $\mathbf{1}^+$−$\mathbf{7}^+$ was efficiently quenched by TEOA, as shown in Table 1, and completely quenched in 5:1 DMF−TEOA solution. Figure 1a illustrates the UV/vis absorption change of the DMF−TEOA solution containing $\mathbf{6}^+$ during irradiation. The new absorption band that grows in during irradiation is attributed to the OER complex **6** because of the similarity to the spectra of $[ClRe(bpy^{\bullet-})(CO)_3]^-$ [9,10] and $[Re(bpy^{\bullet-})(CO)_2\{P(OEt)_3\}_2]$.[12] This identification is also strongly supported by the fact that a very similar absorption spectrum was observed by the flow electrolysis of a MeCN solution containing $\mathbf{6}^+$, as shown in Figure 1b. The quantum yield of the photochemical formation of **6** was calculated using the quanta absorbed by $\mathbf{6}^+$ (ϵ_{365} = 3130 M^{-1} cm^{-1}), which was calculated by considering the internal filtering effect of **6** (ϵ_{365} = 5810 M^{-1} cm^{-1}). The growth in concentration of **6** showed a good linear correlation with the calculated absorbed-light quanta, and the OER formation yield was evaluated as about 2 under either a CO_2 or Ar atmosphere.

Other OER species **1**−**5** and **7** were also accumulated in high yields under the photoreaction conditions. Table 2 shows the peak wavelengths of the UV/vis absorption bands of the OER complexes, the irradiation time (T_{max}), and the absorbance (A_{max}) at the peak wavelength around 505 nm when the absorbance of the OER complexes reached a maximum.

The infrared absorption spectra of **1**−**7** were measured using a combination of the flow electrolysis and FT-IR. As an example, the IR spectra just after the flow electrolysis of an acetonitrile solution containing $\mathbf{6}^+$ and Et_4NClO_4 as electrolyte at various potentials are illustrated in Figure 2. The three isosbestic points in the spectra clearly indicate considerable stability of **6** under an argon atmosphere. The maxima of the CO stretching bands of the OER complexes and their differences between $\mathbf{1}^+$−$\mathbf{7}^+$ and **1**−**7** are summarized in Table 2.

Discussion

The OER species **6** was rapidly produced in quantitative yield and then decreased slowly during irradiation.

(23) The complexes $\mathbf{1}^+$−$\mathbf{7}^+$ and the formate complex were quantitatively analyzed using an HPLC with an ODS column. Details of the HPLC conditions are described in the following reference: Hori, H.; Koike, K.; Ishizuka, M.; Westwell, J. R.; Takeuchi, K.; Ibusuki, T.; Ishitani, O. *Chromatographia* **1996**, *43*, 491−495.

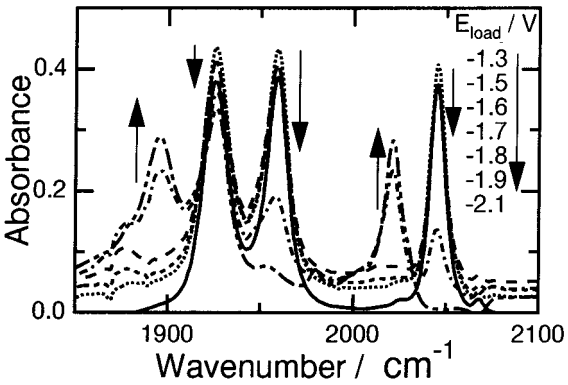

Figure 2. IR spectral change of an MeCN solution containing $\mathbf{6}^+$ (0.52 mM) during electrolysis at various potentials vs $Ag/AgNO_3$ under an Ar atmosphere.

The quantum yield of the photochemical formation of **6** was about 2 under either a CO_2 or Ar atmosphere. This is not surprising, because it has been reported[24] that deprotonation from $TEOA^{\bullet+}$, which should be produced by electron transfer from TEOA to the excited $\mathbf{6}^+$, is very rapid (eq 1) and the product (**8**) is a strong reductant which should be able to reduce another $\mathbf{6}^+$ molecule (eq 2).[10] Similarly to $\mathbf{6}^+$ (Figure 1), isosbestic points were

$$N^{\bullet+}(CH_2CHOH)_3 + TEOA \rightarrow HOCH_2C^{\bullet}HN(CH_2CHOH)_2 + TEOAH^+ \quad (1)$$
8

$$\mathbf{8} + \mathbf{6}^+ \rightarrow HOCH_2CH{=}N^+(CH_2CHOH)_2 + \mathbf{6} \quad (2)$$

observed around 320 nm in the UV/vis absorption spectra of the solutions containing $\mathbf{1}^+$–$\mathbf{5}^+$ and $\mathbf{7}^+$ and TEOA during the generation of the OER species by irradiation. When the yield of the OER species was at a maximum, the absorbances at the absorption maximum around 505 nm of **1**–**5** and **7** were similar to that of $\mathbf{6}^+$ (Table 2). These results strongly suggest that the formation of the OER species is much faster than their decomposition processes under reaction conditions and only minor effects from the ligands are observed on the photochemical formation rate and yield of the OER species.

It is of mechanistic significance to note that reactivities of the OER complexes were strongly affected by PR_3 and X_2bpy. Photochemically produced **1**, **2**, and **7** were extremely stable in a degassed solution *in the dark*: 60–80% still remained even after 10 h, whereas the other OER complexes substantially decomposed in the dark. The decays of **3**–**6** in the degassed solution were found to follow second-order kinetics (Figure 3a). For the kinetic analysis, the molar extinction coefficient of **6** was determined by a flow-electrolysis technique,[25] and the second-order decay rate constant was evaluated as 25.4 M^{-1} s^{-1}. Interestingly, decay of the OER complexes in the dark was enhanced by the introduction of CO_2 in the degassed solution, following the kinetic equation (3), where k_1 and k_2 are the second-order rate constants. Figure 3b depicts the decay of **6** under a CO_2 atmosphere in the dark: the fit is from a nonlinear least-squares analysis using eq 3. It should be noted that k_2 in the presence of CO_2 (23.3 M^{-1} s^{-1})[26] shows good agreement with the second-order decay rate constant (25.4 M^{-1} s^{-1}) of **6** in the degassed solution (*vide supra*). This indicates that the decay of the OER species under a CO_2 atmosphere in the dark involves two different mechanistic channels, *i.e.*, a reaction of the OER species with CO_2 and a second bimolecular process involving reaction between two OER species without the participation of CO_2. In order to evaluate the relative importance of these dark reactions in the photocatalytic CO_2-reduction cycle, we estimated the "yield of CO" on the basis of the assumption that each of the thermal reactions would generate CO quantitatively (eqs 4 and 5). The "yield of CO" at time T was calculated by

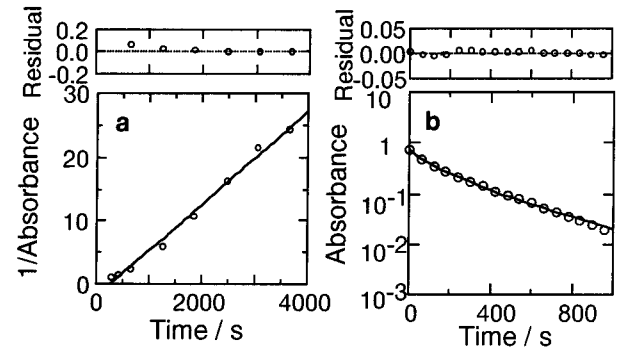

Figure 3. Decay profiles of **6**, which is produced by photochemical reduction of $\mathbf{6}^+$ by TEOA, in the dark: (a) in a degassed solution with the fitting curve using second-order kinetics; (b) under a CO_2 atmosphere with the nonlinear least-squares fitting result using eq 3.

$$-\mathrm{d}[\text{the OER complexes}]/\mathrm{d}t = k_1[\text{the OER complexes}][CO_2] + k_2[\text{the OER complexes}]^2 \quad (3)$$

$$[Re(Me_2bpy^{\bullet-})(CO)_3\{P(OEt)_3\}] + CO_2 \xrightarrow[\text{dark}]{k_1} CO \quad (4)$$
6

$$2[Re(Me_2bpy^{\bullet-})(CO)_3\{P(OEt)_3\}] \xrightarrow[\text{dark}]{k_2,\ CO_2} CO \quad (5)$$

analysis of the time profile for the growth and decay of **6** (*e.g.*, Figure 4) using eq 6 or 7, where T is the time

$$[CO]_{eq4} = \int_0^T k_1[\mathbf{6}][CO_2]\,\mathrm{d}t \quad (6)$$

$$[CO]_{eq5} = \int_0^T k_2[\mathbf{6}]^2\,\mathrm{d}t \quad (7)$$

when the irradiation was stopped. Table 3 summarizes the calculated values of $[CO]_{eq4}$ and $[CO]_{eq5}$ together with the observed CO yields under various conditions (different concentrations of $\mathbf{6}^+$ and different light intensities). The yields calculated by eq 7 ($[CO]_{eq5}$)

(24) Chan, S.-F.; Chou, M.; Creutz, C.; Matsubara, T.; Sutin, N. *J. Am. Chem. Soc.* **1981**, *103*, 369.

(25) λ_{max}/nm (ϵ/M^{-1} cm^{-1}) of **7**: 513 (3500), 482 (2400), 448 (1600), 393 (5200).

(26) The $k_1[CO_2]$ values were experimentally determined as the pseudo-first-order rate constants. The concentration of CO_2 was 0.139 M in the CO_2-saturated DMF–TEOA solution at 25 °C. For determining this, we used the titration method reported by Fujita et al., but a pH meter was employed instead of the indicator dye and pH 9.5 was adopted as the end point of the titration because of the buffer capability of TEOA. Fujita, E.; Szalda, D. J.; Creutz, C.; Sutin, N. *J. Am. Chem. Soc.* **1988**, *110*, 4870. Schmidt, M. H.; Miskelly, G. M.; Lewis, N. S. *J. Am. Chem. Soc.* **1990**, *112*, 3420.

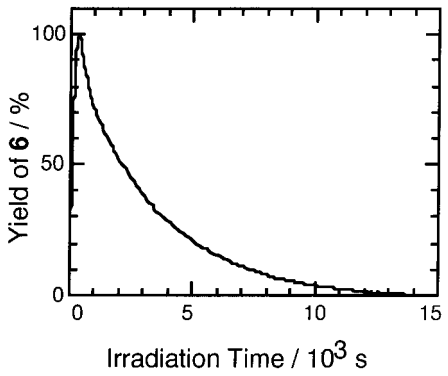

Figure 4. Yield−time curve of **6** in a TEOA−DMF (1:5 v/v) solution during the photocatalyzed reduction of CO_2: [$\mathbf{6}^+$] = 0.26 mM; light intensity 1.27×10^{-8} einstein s^{-1} at 365 nm.

Table 3. Photocatalyzed CO Formation by 6^+ and the Calculated Yields of CO Using Eqs 6 and 7

[$\mathbf{6}^+$]/mM	rel light intensity	irrad time/min	amt of CO/μmol obsd[a]	[CO]$_{eq4}$[b]	[CO]$_{eq5}$[b]
0.069	1	230	0.83	1.91	0.52
0.069	2.0	100	0.37	1.04	0.44
0.196	2.7	240	0.96	2.04	2.21
2.675	2.7	960	52.54	104.5	310.7

[a] A DMF−TEOA solution (5:1 v/v, 4 mL) containing $\mathbf{6}^+$ (2.6 mM) was irradiated using 365 nm monochromic light under a CO_2 atmosphere until **6** was not detected in the solution. [b] The "yield of CO" on irradiation was calculated by the time profile for the growth and decay of **6** (e.g., Figure 4) and eq 6 or 7.

showed a drastic change from the minimum value (0.44 μmol) to the maximum (310.7 μmol), depending on the conditions, a much larger change compared with that of the observed yields. It is of significance to note that the value of [CO]$_{eq5}$ (0.52 μmol) at 0.069 mM of $\mathbf{6}^+$ and at the lowest light intensity is significantly smaller than the observed yield (0.83 μmol), even though the calculated values under the other reaction conditions are always greater than the corresponding observed values. Clearly, there is no direct correlation between the experimental results and [CO]$_{eq5}$. In contrast, the amount of CO formation under various experimental conditions was half that predicted by eq 6 ([CO]$_{eq4}$).

These arguments strongly suggest that the photocatalytic CO_2 reduction mechanism should involve, at least in part, the reaction of the OER species with CO_2 (eq 4) as an essential mechanistic pathway, while eq 5 might play a minor role, if any. The 2-fold difference between the observed and calculated yields of CO suggests that there is a disproportionation process between two intermediate species (I) to give one CO molecule (eq 8) or some competitive reaction pathways which do not give any CO.

$$\mathbf{6} + CO_2 \rightarrow I \xrightarrow{\times 2} CO + 2\mathbf{6}^+ \qquad (8)$$

The mechanism shown in eq 4 is again supported by a good correlation between k_1 and the observed quantum yields of CO formation for the Re(I) complexes used (Table 1). While the complexes ($\mathbf{1}^+$, $\mathbf{2}^+$, and $\mathbf{7}^+$) having low photocatalytic capabilities ($\Phi_{CO} \leq 0.02$) reveal small k_1 values ($< 1.1 \times 10^{-3}$ M^{-1} s^{-1}), much more efficient CO evolution ($\Phi_{CO} = 0.16-0.2$) occurs with $\mathbf{3}^+-\mathbf{6}^+$, the OER species of which can react with CO_2 at much higher rates ($k_1 \geq 5.6 \times 10^{-3}$ M^{-1} s^{-1}).

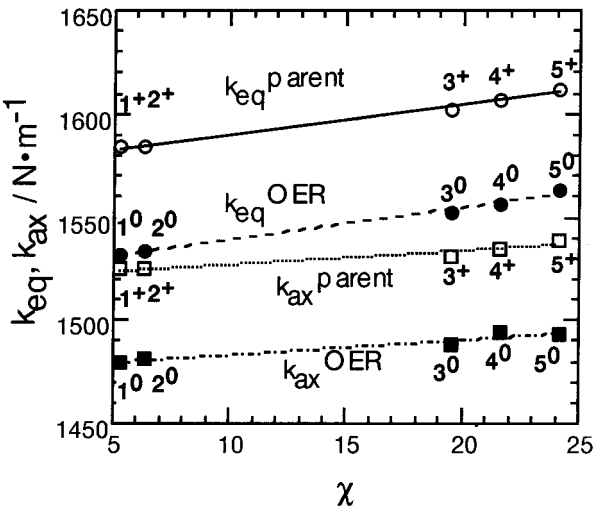

Figure 5. Relationships between the force constants of the ligand CO bonds of **1**−**5** and Tolman's χ.

There are three mechanistic possibilities for the reaction between the OER complexes and CO_2: the OER complexes release one of the ligands to be a coordinatively unsaturated species, which reacts with CO_2, *i.e.*, a dissociative mechanism (eq 9); the OER complexes are electrophilically attacked by CO_2 followed by ligand loss, *i.e.*, an associative mechanism (eq 10); there is an outer-sphere electron transfer reaction from the OER complexes to CO_2 (eq 11).

$$[ReL] \rightleftarrows [Re] + L \xrightarrow{CO_2} [ReCO_2] \qquad (9)$$

$$[ReL] + CO_2 \rightleftarrows [Re(CO_2)L] \rightarrow [ReCO_2] + L \qquad (10)$$

$$[ReL] + CO_2 \rightarrow [ReL]^+ + CO_2^{\bullet -} \qquad (11)$$

Considering the redox potentials of the rhenium complexes (−1.03 to −1.44 V vs $Ag/AgNO_3$ in Table 1) and CO_2 (ca. −2 V vs NHE[27,28]), the driving force of the electron transfer reaction should be too small and eq 11 should be excluded as a possible reaction pathway. Figure 5 illustrates the linear relationships between the force constants of the CO bonds of **1**−**5** and Tolman's χ, which is an indication of the electron-donating ability of the phosphorus ligands.[22,29,30] The good correlation clearly indicates that electron density of the central rhenium systematically varies with the electron-donation ability of the phosphorus ligands; *i.e.*, a stronger electron-withdrawing ligand such as $P(OMe)_3$ lowers the electron density of the rhenium and then the π-back-donation to the CO ligands becomes weaker. If nucleophilic attack of the OER complexes to CO_2 is the rate-determining process, the larger χ of the phosphine ligands would make k_1 smaller. However, there is not such a correlation between k_1 and χ (Figure 6). The cone angle (θ) of the phosphorus ligands possibly affects the rate of the reaction. However, there is also no correlation between θ and k_1 (Table 1). These results suggest that the nucleophilicity of the OER complexes is less important for the reaction with CO_2. It is well-

(27) Haynes, L. V.; Sawer, D. *Anal. Chem.* **1967**, *39*, 332.
(28) Amatore, C.; Saveant, J. M. *J. Am. Chem. Soc.* **1981**, *103*, 5021.
(29) Bartik, T.; Himmer, T.; Schutte, H.-G.; Seevogel, K. *J. Organomet. Chem.* **1984**, *272*, 29.
(30) Tolman, C. A. *Chem. Rev.* **1977**, *77*, 313.

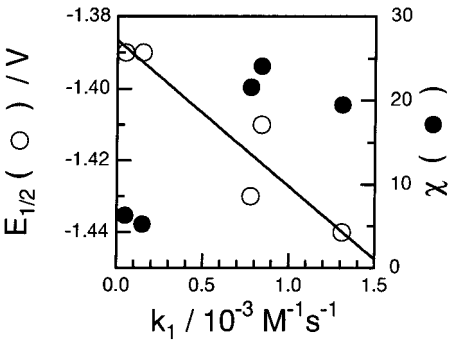

Figure 6. Plots of Tolman's χ and $E_{1/2}$ (redox potentials of **a**/**a**$^+$ vs $Ag/AgNO_3$) vs k_1 (the observed rate of the reaction between the OER complexes and CO_2 in the dark; see text), where **a**$^+$ = **1**$^+$−**5**$^+$.

established from electrochemical investigations that the first reductions of the rhenium bipyridine complexes involve bipyridyl-based one-electron reduction to produce OER species such as $[Re^I(bpy^{\bullet-})(CO)_3Cl]^-$.[7,9−14,31] In the cases of **1**−**7**, the electron inserted into the complexes should also be mainly located on the 4,4′-X_2-bpy ligand. This was supported by the UV/vis absorption spectra of **1**−**7** and the frequency shift of the ν(CO) bands caused by the one-electron reduction of **1**$^+$−**7**$^+$ being similar to those of the reported rhenium complexes (Table 2).[12−14] Consequently, the redox potential of the complexes $E_{1/2}$(**a**/**a**$^+$) (**a** = **1**−**7**) can be used as a measure of the electron-donating ability of the ligand (4,4′-X_2bpy$^{\bullet-}$). Interestingly, the more negative $E_{1/2}$(**a**/**a**$^+$) was, the bigger k_1 was (Figure 6 and Table 1). It is not unreasonable that intramolecular electron transfer from the 4,4′-X_2bpy$^{\bullet-}$ ligand to the central rhenium(I) of the OER species assists in ligand loss. Consequently, these results add some support to the dissociative mechanism.

Reduction of CO_2 to CO requires two electrons. However, it should be pointed out that the available electron from **8**, only reacts to reduce **6**$^+$ to **6** and does not react with other intermediates in the CO_2 reduction process. This is consistent with the observed quantum yield of **2** for the formation of **6**. Therefore, the reduction of the other intermediate(s) in the photocatalytic cycle should occur with another electron source.

Acknowledgment. We acknowledge helpful discussions with Dr. Chyongjin Pac, Kawamura Institute of Chemical Research. This work was supported by the Agency of Industrial Science and Technology of Japan (Development of Global Environment Technology) and the Research Institute of Innovative Technology for the Earth (RITE).

OM970608P

(31) Stor, G. J.; Hartl, F.; Vanoutersterp, J. W. M.; Stufkens, D. J. *Organometallics* **1995**, *14*, 1115−1131.